# Faraday Discussions

Accepted Manuscript


This manuscript will be presented and discussed at a forthcoming Faraday Discussion meeting. All delegates can contribute to the discussion which will be included in the final volume.

**Register now to attend!** Full details of all upcoming meetings: http://rsc.li/fd-upcoming-meetings

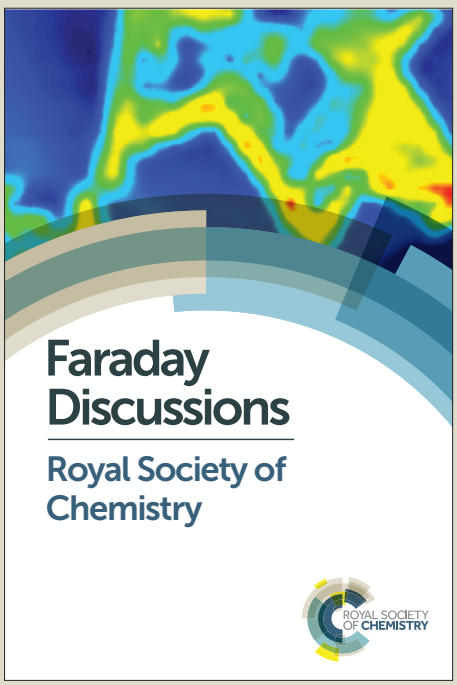


This is an *Accepted Manuscript*, which has been through the Royal Society of Chemistry peer review process and has been accepted for publication.

*Accepted Manuscripts* are published online shortly after acceptance, before technical editing, formatting and proof reading. Using this free service, authors can make their results available to the community, in citable form, before we publish the edited article. We will replace this *Accepted Manuscript* with the edited and formatted *Advance Article* as soon as it is available.

You can find more information about *Accepted Manuscripts* in the Information for Authors.

Please note that technical editing may introduce minor changes to the text and/or graphics, which may alter content. The journal's standard Terms & Conditions and the Ethical guidelines still apply. In no event shall the Royal Society of Chemistry be held responsible for any errors or omissions in this *Accepted Manuscript* or any consequences arising from the use of any information it contains.

ROYAL SOCIETY OF CHEMISTRY

www.rsc.org/faraday_d

Journal Name

RSCPublishing

ARTICLE

# Photoelectrochemical Properties of Porphyrin Dyes with a Molecular Dipole in the Linker

Cite this: DOI: 10.1039/x0xx00000x

Ken T. Ngo[a], Jonathan Rochford[a],* Hao Fan[b], Alberto Batarseh[b], Keyur Chitre, Sylvie Rangan,[c] Robert A. Bartynski[c], and Elena Galoppini[b]*

Received 00th January 2012,
Accepted 00th January 2012

DOI: 10.1039/x0xx00000x

www.rsc.org/

Abstract

The electronic properties of three porphyrin-bridge-anchor photosensitizers are reported with (**1a,e** and **3a,e**) or without (**2a,e**) an intramolecular dipole in the bridge. The presence and orientation of the bridge dipole is hypothesized to influence photovoltaic properties due to variations in the intrinsic dipole at the semiconductor-molecule interface. Electrochemical studies of the porphyrin-bridge-anchor dyes self-assembled at mesoporous nanoparticle $ZrO_2$ films, show that the presence or direction of the bridge dipole does not have an observable effect on the electronic properties of the porphyrin ring. Subsequent photovoltaic measurements at nanostructured $TiO_2$ semiconductor films in dye sensitized solar cells show a reduced photocurrent for photosensitizers **1a** and **3a** containing a bridge dipole. However, cooperative increased binding of the **1a**+**3a** co-sensitized device demonstrates that dye packing overrides any differences due to the presence of the small internal dipole.

## Introduction

The performance of dye sensitized solar cells (DSSCs) is highly dependent upon the efficiency of photoinduced charge-separation and the energy level alignment of the semiconductor/dye interface. This energy level alignment dictates kinetics of the charge transfer step, and influences the open-circuit potential ($V_{OC}$), short-circuit current ($I_{SC}$) and, ultimately, the overall power conversion efficiency ($\eta$) in a photovoltaic device.[1,2] While there are numerous interfaces present in a DSSC device, as illustrated in Figure 1, we are particularly interested in the semiconductor/dye interface where molecular design can be leveraged to optimize thermodynamic and kinetic properties of charge transfer. Examples of strategies that are pursued to tune the energy level alignment at the semiconductor/molecule interface include, synthetic design of the dye (e.g., perfluorination, metallic-ion substitution, push-pull design),[3,4,5,6-8] manipulating molecular orientation on the surface[3,9] and co-depositing two or more organic species.[10]

A concept that is attracting increasing attention is that the energy level alignment of any interface at equilibrium is shifted, relative to its component native band edges, due to an *intrinsic interface dipole* (IID).[3,4,11-15] For example, at the semiconductor/molecule interface, the IID effect has been shown responsible for attenuation of the conduction-band edge populations of $TiO_2$ and the LUMO of surface bound organic semiconductors.[16] This has been explained by equilibration of the $TiO_2$ semiconductor Fermi level with the adsorbed molecule's redox potentials. As the semiconductor/molecule IID is principally dependent upon the molecular ionization energies, numerous studies have aimed at tuning ionization energies,[3,4,8,17-19] although other factors also play a role such as molecular orientation and buffer effects, and photoinduced dipole moment changes.[20]

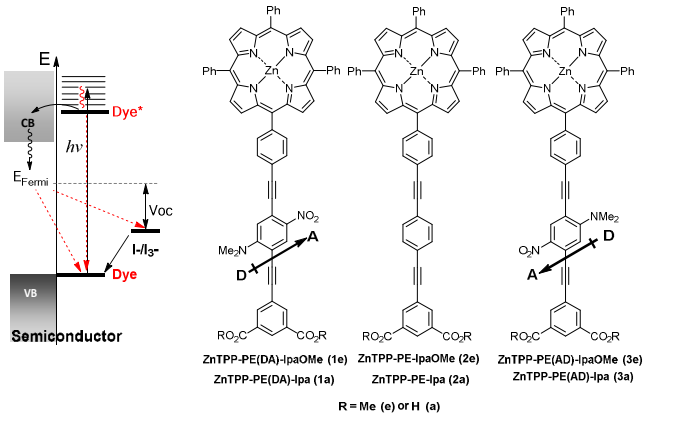


**Figure 1**. ***Left:*** Qualitative diagram of main heterogeneous charge transfer events in a DSSC. ***Right:*** Molecular structures of the ZnTPP dyes studied here,

incorporating the phenylenethynylene (PE) linker, with and without the DA or AD dipole, and the dimethylisophthalate ester (IpaOMe, **e**) or isophthalate acid (Ipa, , **a**) anchor units.

Molecular design is an excellent opportunity to probe the dipole effect concept, and we recently introduced a promising approach by incorporating an internal electric dipole moment within the bridge framework of a chromophore−bridge−anchor molecular architecture. We recently reported the synthesis of ZnTPP rigid-rod dyes **1-3**, shown in Fig. 1[21] where the dipole in the bridge is created by introducing donor-acceptor (DA) or acceptor-donor (AD) substituents, where D = *N,N*-dimethylamino and A = nitro group (Fig. 1). Because the porphyrin macrocycle is almost perpendicular to the rigid-rod bridge, the electronic properties (HOMO-LUMO gap) of the ZnTPP porphyrin chromophore head group are decoupled from the bridge dipole, as determined by UV-Vis absorption, fluorescence emission and redox potentials.[21] This molecular design allows us to associate any difference in energy level alignment at the semiconductor/molecule interface with the dipole orientation in the bridging unit and its influence on the IID effect. In a proof-of concept experiment we recently reported the UV photoemission spectroscopy (UPS) study of **1a**, **2a** and **3a** bound to a ZnO(11−20) single crystal surface to probe the dipole effect on the alignment of the frontier orbital energies with respect to the band edges of the semiconductor.[22] It was determined that the interfacial dipole layer that is formed upon binding to ZnO(11−20) single crystal establishes a potential difference that shifts the HOMO and LUMO levels of the dye with respect to those of the semiconductor.[22] Furthermore, the direction and magnitude of the shift was consistent with that predicted by a simple parallel-plate capacitor model.[22] The magnitude of the shift, i.e. (±) ~100 meV, was small. This was expected, because the internal dipole is not aligned with the surface normal, and the molecules do not bind perpendicularly to the semiconductor.[22]

In this paper we report the electrochemical and photoelectrochemical properties of **1-3** in solution and bound to nanostructured $TiO_2$ and $ZrO_2$ films. First, we wanted to study any changes induced by the bridge dipoles. Second, we wanted to probe if the small dipole effect observed on a single crystal surface could be observable on nanostructured metal oxide surfaces.

## Results and discussion

### Computational analysis

Density functional theory (rB3LYP/6-31g**/PCM-acetonitrile) was employed to get a theoretical insight into the energies and distributions of the frontier molecular orbitals for each of the porphyrin dyes. Select molecular orbital energies and images are presented in Figure 2. Immediately apparent is that the porphyrin based HOMO levels are identical for all dyes and are completely decoupled from the bridging unit as anticipated. The LUMO level for porphyrin **2a** is also based on the porphyrin macrocycle and is typical of a ZnTPP chromophore. The bridge based $\pi^*$ orbital on **2a** occurs at higher energy as the LUMO+2 orbital, again electronically decoupled from the porphyrin macrocycle. In contrast, introduction of the DA/AD dipoles in the bridging units of porphyrins **1a** and **3a** lowers the energy of the bridge based $\pi^*$ orbital due to the strongly withdrawing nitro substituent resulting in this energy level now being the LUMO for each of these dyes. Accordingly, the porphyrin based $\pi^*$ orbital now becomes the LUMO+1 level for both **1a** and **3a**. It should be noted that this LUMO+1 level is electronically and energetically equivalent to the LUMO level of porphyrin **2a** which lacks the dipole substituents. These observations are consistent with the trend in redox potentials discussed below.

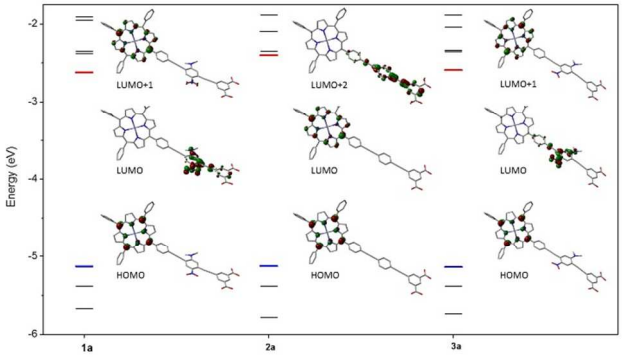


**Figure 2.** Molecular orbital energy level diagram for porphyrin dyes **1a**, **2a** and **3a** calculated using DFT (rB3LYP/6-31g**/acetonitrile PCM). HOMO and LUMO levels are highlighted in blue and red, respectively. Electron occupancy is not displayed, and only select frontier orbital images are included for clarity.

### UV-Vis electronic absorption spectroscopy.

The UV−vis absorption and fluorescence emission spectra for each of the porphyrins was recently reported.[21,22] The similarity of absorption and emission spectra confirmed that the electronic properties of the ZnTPP core were unaffected by the nature of the bridging and anchoring group. All of the dyes exhibit standard features of a ZnTPP chromophore with a strongly absorbing Soret band ($S_0 \rightarrow S_2$) centered at 422 nm ($\varepsilon \sim 5 \times 10^5$ $M^{-1}$ $cm^{-1}$) and weaker Q-bands ($S_0 \rightarrow S_1$) centred at 556 nm and 597 nm ($\varepsilon \sim 1 - 2 \times 10^4$ $M^{-1}$ $cm^{-1}$).[21-23] Absorption spectra for the chemisorbed dyes **1a**, **2a** and **3a** recorded on transparent cover glass/$TiO_2$ thin films are, for the most part, consistent with the solution phase spectra reported earlier. However, a slight broadening on the high energy side of the Soret bands is observed for all dyes (including a 1:1 mixture of dyes **1a**+**3a**) most likely due to H-aggregation upon self-assembly at the semiconductor/dye interface.[23]

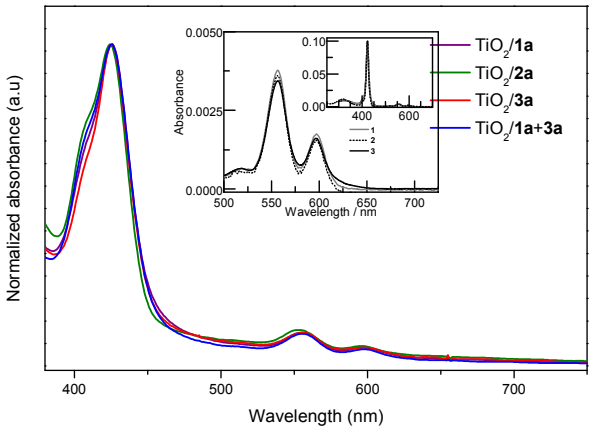


**Figure 3.** Absorption spectra of **1a**, **2a** and **3a** and **1a+3a** chemisorbed on optically transparent $TiO_2$ films. ***Inset:*** Absorption spectra of **1e-3e** in acetonitrile solution (data taken from ref. 21)

## Electrochemical properties

Cyclic voltammetry was carried out on the methyl esters of all porphyrins to investigate their potential for application in a $TiO_2$ based DSSC device and to also determine the influence of the bridge dipole on dye redox potentials. The cyclic voltammetry experiments in solution were conducted with the more soluble esters, since carboxylic acids may decarboxylate or adsorb on the electrodes during the experiments. Redox potentials of the ester derivatives **1e**, **2e** and **3e** recorded in 1,2-dichloroethane are summarized in Table 2 and voltammograms are available in the supporting information Figure S1. All porphyrins show two reversible oxidations assigned to formation of the ZnTPP radical cation and cation, respectively. Radical cation formation occurs at +1.0 V vs. NHE for all porphyrins, which provides sufficient driving force for iodide redox mediator oxidation in a DSSC device ($2I^- \rightarrow I_2^{\bullet-}$, $E$ ~ +0.93 V vs. NHE).[24-26] Additional irreversible oxidation processes are observed for porphyrins **1e** and **3e** most likely due to the electron rich *N,N*-dimethylamino benzene moiety of the dipole bridge. Similarly, all porphyrins display two quasi reversible reductions, assigned to the ZnTPP radical anion and anion, respectively. An additional quasi-reversible reduction process is observed at more positive potential for **1e** (-0.87 V) and **3e** (-0.88 V) assigned to one-electron reduction of the low lying dipolar bridge π* based orbital. The relatively positive nature of this reduction process is no doubt resulting from the strongly electron withdrawing nitro benzene component of the dipole-containing bridge as confirmed by DFT analysis as well as cyclic voltammetry of the independent bridging unit (Fig. S2). The more negative potential required to generate the porphyrin radical anion of **1e** (-1.39 V) and **3e** (-1.43 V) relative to **2e** (-1.17 V) is ascribed to the fact that the former compounds are already reduced by one electron at the bridge prior to reduction of the porphyrin macrocycle.

**Table 2.** Electrochemical properties of the porphyrin dyes **1e-3e**.[ab]

| Dyes | $E_{ox}$ (V vs. NHE) | $E_{red}$ (V vs. NHE) |
|---|---|---|
| **1e** | +1.78[c], +1.68[c], +1.39, +1.00 | -0.87, -1.39[d], -1.56[d], -1.78[d] |
| **2e** | +1.40, +1.00 | -1.17, -1.53[d], -1.74[d] |
| **3e** | +1.81[c], +1.69[c], +1.43, +1.00 | -0.88, -1.43[d], -1.56[d], -1.75[d] |

[a] ±0.005 V [b] Recorded in 0.1 M $Bu_4NPF_6$ 1,2-dichloroethane electrolyte. [c] $E_{pa}$ [d] $E_{pc}$

Cyclic voltammetry was also conducted on thin films of the bound porphyrin compounds, consisting of FTO/mesoporous-$ZrO_2$/porphyrin carboxylic acids **1a-3a** working electrodes to investigate for consistency of solution phase voltammetry with respect to the surface bound porphyrins. The insulating $ZrO_2$ metal oxide is more suitable for these studies as its redox chemistry lies outside the potential window of the electrolyte solution. This allows for uninterrupted observation of both porphyrin oxidation and reduction processes at the metal-oxide/photosensitizer interface. If $TiO_2$ electrodes were used reduction of its conduction band would saturate the voltage response beyond -0.5 V precluding observation of the bridge and ZnTPP reduction processes. As evident in Figure 4 a similar redox profile is observed at the $ZrO_2$ interface as observed in solution. For example, although there is a slight positive shift in the first oxidation potential this is consistent for all porphyrins. Both porphyrins **1a** and **3a** clearly show reduction of the dipolar bridge unit at *ca.* -0.9 V in the solid state which is absent for the reference PE-bridged dye **2a**.

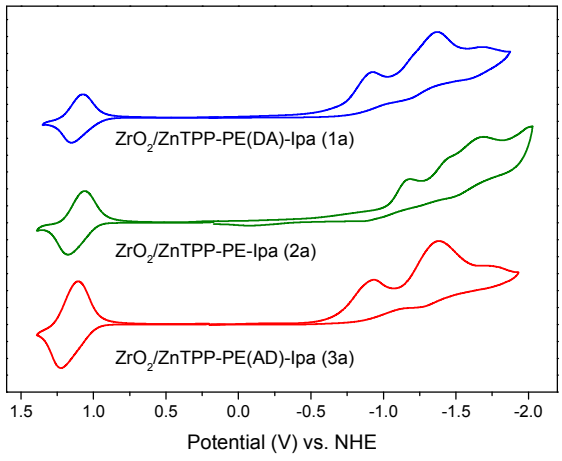


**Figure 4.** Cyclic voltammetry of porphyrins **1a**, **2a** and **3a** recorded using chemisorbed FTO/$ZrO_2$/porphyrin working electrodes in a 0.1 M $Bu_4NPF_6$ acetonitrile electrolyte solution (scan rate = 0.1 V $s^{-1}$).

## Photovoltaic studies

Photocurrent density-voltage (*J-V*) experiments were conducted for all three porphyrins **1a-3a** using standard DSSC fabrication

methods (FTO/$TiO_2$/dye/($I_3^-$/$I^-$)/Pt/FTO) and are presented in Figure 5.

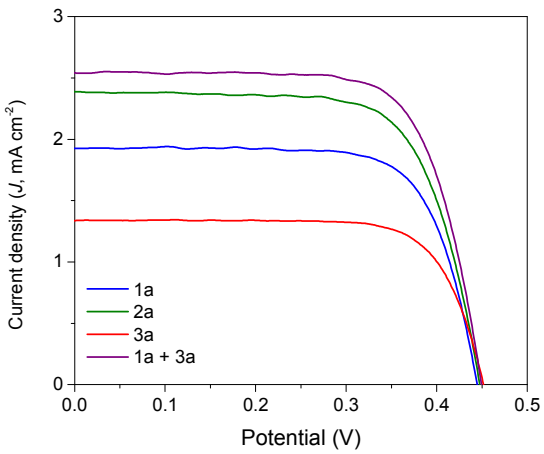


**Figure 5.** Photocurrent–voltage (*J-V*) plots of the porphyrin DSSC devices recorded under AM 1.5G simulated irradiation.

The photosensitizer **2a** which lacks a dipole on the PE bridge shows a greater power conversion efficiency in comparison to the **1a** and **3a** dyes, the latter displaying the lowest overall efficiency. To investigate whether the bridge dipole inherently gives a lower overall performance a co-sensitized DSSC device was also fabricated using a 1:1 sensitizing solution of porphyrins **1a** and **3a**. Surprisingly, upon co-adsorption of both **1a** and **3a** dyes to the same FTO/$TiO_2$ photoanode a significant improvement in efficiency is observed, almost twice that of the independent **3a** dye and surpassing that of the **2a** dye. The nature of this increase in efficiency, from a device perspective, is primarily due to an increase in the photocurrent density as all DSSCs show equal open-circuit potential ($V_{OC}$ = 0.45 V) and similar fill factors (0.70 to 0.74). A subsequent binding study analysis showed an almost two-fold increase in surface coverage for the co-sensitized DSSC relative to the independent dyes which had comparable surface coverage. This observation is consistent with the trend observed for the independent photosensitizers and implies that the increase in photocurrent for the co-sensitized DSSC is related to its increased surface packing, rather than the direct result of any bridge-dipole effect. Furthermore, ground state redox potentials of the FTO/$ZrO_2$/porphyrin carboxylic acid **1a-3a** working electrodes are consistent with solution phase cyclic voltammetry precluding any significant change in electronic structure upon adsorption in the mesoporous structure. The photovoltaic performance of each DSSC device is summarized in Table 2 which includes short-circuit current density (*J*sc), open-circuit voltage (*V*oc), fill factor (*FF*), and power conversion efficiency (η) data.

**Table 2**. Photovoltaic performance data of the four DSSC devices.

| Dyes | Γ ($10^{-8}$ mol $cm^{-2}$) | $V_{OC}$ (mV) | $J_{SC}$ (mA $cm^{-2}$) | *FF* | η (%) |
|---|---|---|---|---|---|
| **1a** | 4.74 | 0.45 | 1.93 | 0.73 | 0.63 |
| **2a** | 3.47 | 0.45 | 2.39 | 0.70 | 0.75 |
| **3a** | 3.37 | 0.45 | 1.34 | 0.74 | 0.45 |
| **1a+3a** | 5.79 | 0.45 | 2.54 | 0.72 | 0.82 |

Light source: 100 mW $cm^{-2}$ AM 1.5G simulated solar light. Working area: 0.36 $cm^2$. Thickness: 4 um active layer. Electrolyte: 0.06 M LiI, 0.03 M $I_2$, 0.6 M 1,2-dimethyl-3-propylimidazolium iodide (DMPII), 0.5 M 4-tertbutylpyridine (TBP) in acetonitrile solution.

## Conclusions

The electrochemical and photoelectrochemical properties of rigid-rod porphyrins with (**1a,e** and **3a,e**) or without (**2a,e**) an intramolecular dipole in the bridge were studied in solution and bound to nanostructured nanoparticle films ($TiO_2$ and $ZrO_2$). The experiments confirmed that the presence or direction of the bridge dipole does not change the electronic properties of the porphyrin ring. Second, on nanostructured semiconductor films, the differences in packing that are caused by the bridge substitution override any electronic differences due to the presence of the small internal dipole, whereas a dipole effect was clearly observable on monolayers of **1a-3a** on single crystal semiconductors.[22] Current work is devoted to address difference in surface packing and synthesize a new class of compounds with larger dipoles.

## Experimental section

### Analytical measurements

Cyclic voltammetry was conducted on a CH Instruments 620D potentiostat for all complexes. A standard three electrode cell was used with a supporting electrolyte of 0.1 M $Bu_4NPF_6$ in spectrophotometric grade 1,2-dichloroethane under an atmosphere of argon. The electrode assembly consisted of a glassy carbon disc working electrode (3-mm diameter), a Pt wire counter electrode and a non-aqueous reference electrode to minimize IR drop. The latter consisted of a Ag wire in the same 0.1 M $Bu_4NPF_6$ 1,2-dichloroethane electrolyte but separated by a porous Vycor frit. The ferricenium/ferrocene redox couple was used as a pseudo reference and was added to each porphyrin electrolyte solution at the end of every experiment for in-situ calibration. For electrochemical analysis of chemisorbed FTO/$ZrO_2$/porphyrin assemblies the FTO conductive glass was used as the working electrode in place of glassy carbon and 0.1 M $Bu_4NPF_6$ acetonitrile electrolyte was used as solubility in acetonitrile was no longer a limiting factor. FTO electrodes were typically of dimensions 1 cm x 2 cm x 2.2 mm with an active $ZrO_2$/porphyrin area of 1 cm x 2 cm. FTO/$ZrO_2$ electrodes were prepared by a single doctor blade

deposition using the commercial Zr-Nanoxide Z/SP paste followed by sintering at 450 °C and sensitization for 3 hours at room temperature (0.2 mM dye solution in methanol).

### Computational analysis

Geometry optimization was first carried out using density functional theory (DFT) with the rB3LYP hybrid exchange-correlation functional[27,28] and 6-31g** basis set[29,30] for all atoms as implemented in the Gaussian '09 program[31] using the polarizable continuum model (PCM) with the dielectric constant of acetonitrile.[32] A vibrational frequency analysis coupled with the PCM model was carried out in order to confirm the minimum-energy geometry in solution.

### Fabrication of DSSCs and photovoltaic measurements

All DSSCs were prepared from a commercial Solaronix test cell kit. The photoanode consisted of 2 cm x 2 cm x 2.2 mm FTO glass (7 Ω $cm^{-2}$) with a 0.36 $cm^2$ deposited area of $TiO_2$ (Solaronix part # 74101). The electrodes were sintered for 30 min at 450°C and cooled to 80°C prior to dye sensitization for 3 hours at room temperature (0.2 mM dye solution in methanol). The photoanode was assembled with a pre-drilled FTO/Pt counter electrode (Solaronix part # 74201) and sealed together with a 60 µm thick Surlyn® spacer (Solaronix part #74301). The redox mediator solution (0.06 M LiI, 0.03 M $I_2$, 0.6 M 1,2-dimethyl-3-propylimidazolium iodide, and 0.5 M 4-tert-butylpyridine in acetonitrile) was introduced through the pre-drilled counter electrode by vacuum back-filling. For photovoltaic (*I-V*) measurements the assembled DSSCs were connected to a CH 760D potentiostat in linear sweep voltammetry mode. A Newport Oriel 100 W Xe arc lamp was used with an AM 1.5 global filter to simulate the solar spectrum. Light intensity was calibrated at 100 mW $cm^{-2}$ using a reference Si photodiode. The percentage power conversion efficiency ($\eta$) was calculated according to equation 1:

$$\eta = \frac{P_{out}}{P_{in}} \times 100 = \frac{J_{SC}\, V_{OC}\, FF}{I_0} \times 100 \qquad (1)$$

where $J_{SC}$ is the short-circuit current density (mA $cm^{-2}$), $V_{OC}$ is the open-circuit voltage (V), *FF* is the fill-factor and $I_0$ the light flux (100 mW $cm^{-2}$).

### Acknowledgements

Funding by the Division of Chemical Sciences, Geosciences, and Biosciences, Office of Basic Energy Sciences of the U.S. Department of Energy through Grant DE-FG02-01ER15256, is gratefully acknowledged. A. B. thanks Rutgers University Newark for the Summer 2013 FASN Dean's Undergraduate Research Fellowship and the Chemistry Department for the 2014 Ian Fryer Memorial Award. NSF Award MRI 1229030 is acknowledged for the NMR instrumentation necessary for the characterization of **1-3**.

## Notes

[a]Department of Chemistry, University of Massachusetts Boston, 100 Morrissey Boulevard, Boston, MA 02125, United States.
[b]Department of Chemistry, Rutgers University, 73 Warren Street, Newark, NJ 07102 United States.
[c]Department of Physics and Astronomy and Laboratory for Surface Modification, Rutgers University, 136 Frelinghuysen Road, Piscataway, NJ 08854, United States.

**Electronic Supplementary Information (ESI) available:** Full citation for reference 31, cyclic voltammograms of porphyrins **1e**, **2e** and **3e**, cyclic voltammogram of dipole-containing bridge intermediate, cartesian coordinates of geometry optimized structure for **1a**.

## References

1. D. Cahen, G. Hodes, M. Grätzel, J. F. Guillemoles, I. Riess, I. *J. Phys. Chem. B* 2000, **104**, 2053.
2. A. Wilke, J. Endres, U. Hormann, J. Niederhausen, R. Schlesinger, J. Frisch, P. Amsalem, J. Wagner, M. Gruber, A. Opitz, A. Vollmer, W. Brutting, A. Kahn, N. Koch, *Appl. Phys. Lett.* 2012, 101.
3. G. Heimel, F. Rissner, E. Zojer, *Adv. Mater.* 2010, **22**, 2494.
4. A. Kahn, N. Koch, W. Y. Gao, *J. Polym. Sci. Pol. Phys.* 2003, **41**, 2529.
5. F. H. Li, Y. Zhou, F. L. Zhang, X. J. Liu, Y. Q. Zhan, M. Fahlman, *Chem Mater* 2009, **21**, 2798.
6. S. Duhm, G. Heimel, I. Salzmann, H. Glowatzki, R. L. Johnson, A. Vollmer, J. P. Rabe, N. Koch, *Nature Mater.* 2008, **7**, 326.
7. S. Duhm, Q. Xin, N. Koch, N. Ueno, S. Kera, *Org Electron* 2011, **12**, 903.
8. Niederhausen, J.; Amsalem, P.; Frisch, J.; Wilke, A.; Vollmer, A.; Rieger, R.; Mullen, K.; Rabe, J. P.; Koch, N. *Phys Rev B* 2011, *84*.
9. Y. L. Huang, W. Chen, F. Bussolotti, T. C. Niu, A. T. S. Wee, N. Ueno, S. Kera, *Phys. Rev. B* 2013, 87.
10. F. Rissner, D. A. Egger, L. Romaner, G. Heimel, E. Zojer, *ACS Nano* 2010, **4**, 6735.
11. D. Cahen, A. Kahn, *Adv. Mater.* 2003, **15**, 271.
12. J. Hwang, A. Wan, A. Kahn, *Mat. Sci. Eng. R* 2009, **64**, 1.
13. H. Ishii, K. Sugiyama, E. Ito, K. Seki, *Adv. Mater.* 1999, **11**, 972.
14. N. Koch, *Phys. Status Solidi-R* 2012, **6**, 277.
15. H. Vazquez, F. Flores, A. Kahn, A. *Org. Electron.* 2007, **8**, 241.
16. M. T. Greiner, M. G. Helander, W.-M. Tang, Z.-B. Wang, J. Qiu, Z.-H. Lu, *Nature Mater.* 2012, **11**, 76.
17. F. H. Li, Y. Zhou, F. L. Zhang, X. J. Liu, Y. Q. Zhan, M. Fahlman, *Chem. Mater.* 2009, **21**, 2798.
18. S. Duhm, G. Heimel, I. Salzmann, H. Glowatzki, R. L. Johnson, A. Vollmer, J. P. Rabe, N. Koch, *Nature Mater.* 2008, **7**, 326.
19. S. Duhm, Q. Xin, N. Koch, N. Ueno, S. Kera, *Org. Electron.* 2011, **12**, 903.
20. K. Hu, K. C. D. Robson, E. E. Beauvilliers, E. Schott, X. Zarate, R. Arratia-Perez, C. P. Berlinguette, G. J. Meyer *J. Am. Chem. Soc.* 2014, **136**, 1034.

21. K. Chitre, A. Batarseh, A. Kopecky, H. Fan, H. Tang, R. Lalancette, R. A. Bartynski, E. Galoppini *J. Phys. Chem. B,* 2015 Article ASAP.
22. S. Rangan, A. Batarseh, K. Chitre, A. Kopecky, E. Galoppini, R. A. Bartynski *J. Phys. Chem. C* 2014, **118**, 12923.
23. J. Rochford, E. Galoppini *Langmuir* 2008, **24**, 5366.
24. G. Boschloo, A. Hagfeldt, *Acc. Chem. Res.* 2009, **42**, 1819.
25. J. G. Rowley, B. H. Farnum, S. Ardo, G. J. Meyer, *J. Phys. Chem. Lett.* 2010, **1**, 3132.
26. J. H. Baxendale, P. L. T. Bevan, D. A. Stott, *Trans. Faraday Soc.* 1968, **64**, 2389.
27. A. D. Becke, *J. Chem. Phys.* 1993, **98**, 5648.
28. C. T. Lee, W. T. Yang and R. G. Parr, *Phys. Rev. B* 1988, **37**, 785.
29. P. C. Hariharan, J. A. Pople, *Theor. Chim. Acta* 1973, **28**, 213.
30. M. M. Francl, W. J. Pietro, W. J. Hehre, J. S. Binkley, M. S. Gordon, D. J. Defrees, J. A. Pople, *J. Chem. Phys.* 1982, **77**, 3654.
31. Frisch M. J. et al., Gaussian 09, (2009) Gaussian Inc., Wallingford, CT.
32. J. Tomasi, B. Mennucci, R. Cammi, *Chem. Rev*. 2005, **105**, 2999.